RESEARCH ARTICLE

Degradation of Chloridazon in an Aqueous Environment Using TiO_2/Ag as a Synthesized Nano Photocatalyst Using Central Composite Design

Aref Shokri[1,2]*, Meisam Abdolkarimi-Mahabadi[3], Fariba Soleimani[4]

[1]*Jundi-Shapur Research Institute, Jundi-Shapur University of Technology, Dezful, Iran*

[2]*Department of Chemical Engineering, Amirkabir University of Technology, Tehran 15875-4413, Iran*

[3]*Department of Chemical Engineering, Tafresh University, Tafresh 79611-39518, Iran*

[4]*Razi Chemistry Research Center (RCRC), Shahreza Branch, Islamic Azad University, Isfahan, Iran*

ARTICLE INFO

Article History:
Received 2021-06-25
Accepted 2022-03-30
Published 2022-06-30

Keywords:
Chloridazon,
TiO_2/Ag nano photocatalyst,
Photocatalytic degradation,
Central Composite Design (CCD),
Batch photo reactor.

ABSTRACT

In this study, TiO_2/Ag nano photocatalyst was synthesized by sol-gel method and used for degradation of Chloridazon (CLZ) in aqueous media. The prepared catalyst was characterized using powder X-ray diffractometry (XRD), Fourier transform infra-red (FTIR), and field emission scanning electron microscopy (FE-SEM) techniques. The Crystallite sizes of pure TiO_2 and Ag/TiO_2 nanoparticles were 20 and 60 nm, respectively. The Central Composite Design (CCD) was employed for experimental design and statistical analysis of independent operational parameters. According to the results of Response Surface Methodology (RSM) plots of Design-Expert software, the optimal conditions for each critical variable were as the follows: time at 113 min, pH at 6.8, initial concentration of CLZ at 40 mg/l, and catalyst concentration at 0.83gr/l. The maximum effectiveness in the experimental and predicted CLZ removal was 94.2 and 93.5%, respectively. The outcomes of Analysis of variance (ANOVA) demonstrated high determination coefficient quantities (R^2 = 0.9997, Predicted R^2=0.9989, and Adjusted R^2=0.9994) which validated the reliability of the second-order regression model.

How to cite this article
Abdolkarimi M., Soleimani F., Shokri A. Degradation of Chloridazon in an Aqueous Environment Using TiO_2/Ag as a Synthesized Nano Photocatalyst Using Central Composite Design. J. Nanoanalysis., 2022; 9(2): 123-136.
DOI: 10.22034/jna.2022.1934052.1262.

INTRODUCTION

Because of the widespread and extreme applications, pesticides are considered highly used micropollutants which are applied for eliminating different types of insects and weeds to inhibit plant diseases. Even though the major objective of the application of pesticides is increasing the efficiency of agricultural products, the presence of different environmental and human-related adverse effects due to their application is inevitable. According to the various types of pesticides and their half-life, they remain, collect and convey to water and soil for long time. The water-solubility, poisonous nature, and low biodegradability of pesticides can result in ecological contamination because of penetration into both groundwater and surface water. Generally, water sources that are in proximity of agricultural regions include relatively high concentrations of pesticide residuals, as a result, application of such water sources can likely pose significant hazards to human beings [1-2].

One of the well-known pesticides related to the pyrazinone category is chloridazon (5-amino-4-chloro-2-phenyl-3(2H)-pyridazinone). In order to fight against the broad-leaved weeds of beet cultivars as a barricade to the photosynthesis process after and before planting the sugar beets, chloridazon is utilized. Due to the inadequate octanol-water partitioning coefficient (K_{ow}) and significant organic

* Corresponding Author Email: *aref.shokri3@gmail.com*

Table.1. properties of chloridazon.

Properties	Information
Chemical name	chloridazon (5-amino-4-chloro-2-phenyl-3(2H)-pyridazinone)
Synonym	Pyrazon
Molecular formula	$C_{10}H_8ClN_3O$
Vapor pressure	4.50×10^{-7} mmHg at 20 °C
Half-life (d)	105
Appearance	Colorless, Crystalline
K_{oc}	89-340
Dissociation constant pK_a	3.38
Log K_{ow}	1.2
Density (kg/l)	1.54
Water solubility (mg/l)	422
Molecular weight (g/mol)	221.6

carbon-water partitioning coefficient (K_{oc}) of CLZ, it can readily transfer to different environments. As a result, CLZ possesses a significant capacity to penetrate into both groundwater and surface water sources [2]. However, chloridazon elimination from water has not been exhaustively investigated. In limited explorations, for the elimination of CLZ, ozonation [3], photolysis with TiO_2 [4], and adsorption [5] have been used and the elimination effectiveness was completely different, varying from 5% to 100%. Moreover, except Azaari et al. [6] who studied the feasible side-products of CLZ decomposition throughout photolysis with TiO_2, the aforementioned areas are not adequately explored. Hence, additional investigation of CLZ elimination from water resources is essential. Lately, different explorations suggested that advanced oxidation processes (AOPs) are highly effective approaches for the remediation of different pesticide-driven wastewater sources. These processes are remarkably dependent upon the generation of non-selective and powerful $OH^{\bullet}$ radicals by decomposition of H_2O_2 which can effectively treat wastewaters. In comparison with biological and chemical methods, AOPs not only do not generate significant quantities of sludge but also are not based on phase-changing approaches, hence can completely and effectively minimalize different types of recalcitrant contaminants [7-8].

Although using simple photocatalysts such as TiO_2 has many benefits, however, the electron-hole recombination is a disadvantage of TiO_2 nanoparticles during organic materials degradation lead to the lower rate of photocatalysis. The photocatalytic efficacy of nano TiO_2 for degradation of organic pollutants could be increased by depositing metal ions onto TiO_2 surface. It has proven that the electron-hole recombination limitation of TiO_2 nanoparticles within the degradation of organic materials can be reduced by decorated silver (Ag) nanoparticles over the surface of TiO_2. Photo deposition, hydrothermal, co-precipitation, sol-gel, and impregnation are some of the methods which have been used for synthesizing silver-doped TiO_2 with various morphologies [9-11]. Each synthesizing approach has certain pros and cons regarding its preparation process and operational efficiencies. The variation in the photocatalytic activity of Ag/TiO_2 produced by various approaches can originate from thermal remediation throughout the photocatalyst preparation, dosage of silver loading in the ultimate photocatalyst, nanometer-scale particle size, and the oxidation state of silver on the titanium dioxide surface [12-13]. Chen et al. [14] synthesized $Ag@TiO_2$ nanocomposite for degradation of Rhodamine B. The obtained results indicated the higher photocatalytic efficiency of $Ag@TiO_2$ composite compared to TiO_2 nanoparticles. Ag-modified TiO_2 photocatalyst has been used for the degradation

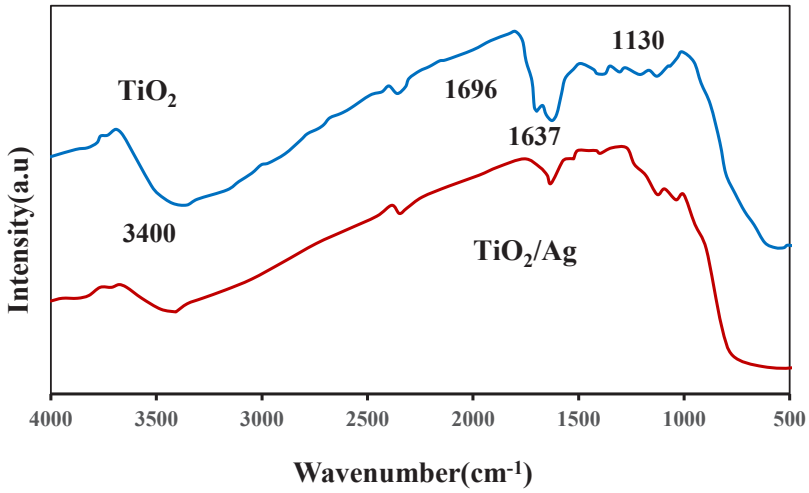

Fig. 1. FT-IR Analysis of TiO_2 and TiO_2/Ag nano photocatalyst.

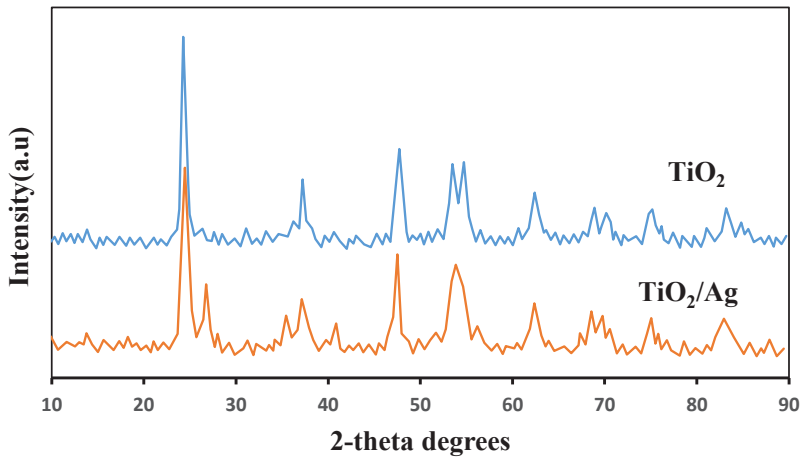

Fig. 2. XRD patterns of (a) TiO_2 nanoparticles, and (b) TiO_2/Ag nanocomposite.

of Indigo carmine under visible light irradiation [15]. Khanna and Shetty [16] synthesized Ag/TiO_2 core-shell for degradation of azo dyes. Tahir et al. [17] evaluated the capacity of Ag/TiO_2 nano photocatalyst for degradation of methylene blue. Results exhibited that 90% of methylene blue was degraded within 40 min of irradiation along with Ag/TiO_2 composite. Leong et al. [18] enhanced the degradation efficiency of TiO_2 nanoparticles toward amoxicillin and 2,4-dichlorophenol by deposition of Ag nanoparticles onto the 100% anatase TiO_2 surface. However, there is no study about the application of Ag/TiO_2 nano photocatalyst for the degradation of CLZ in an aqueous environment.

In this work, the TiO_2/Ag nano photocatalyst was prepared and characterized using XRD, FE-SEM, and FT-IR, techniques and it was applied for the degradation of CLZ. The CCD, as one of the most popular branches of RSM, was employed to explore the influence of four independent parameters including treatment time, pH, initial concentration of CLZ, and concentration of photocatalyst on the efficiency of CLZ removal.

EXPERIMENTAL

Materials

Titanium tetraisopropoxide (TTIP, 98%), Sodium citrate tribasic dihydrate ($C_6H_5Na_3{\cdot}2H_2O$, were purchased from Aldrich. Silver nitrate ($AgNO_3$), nitric acid (HNO_3), ethanol, sulfuric acid (H_2SO_4, 99%) and sodium hydroxide were supplied from Merck. Titanium dioxide P25 Degussa (99.5%) was supplied from Nippon Aerosil Co. Ltd. from Osaka, Japan.

The chloridazon pesticide is supplied from the product Pyrazon commercially, containing 65% of

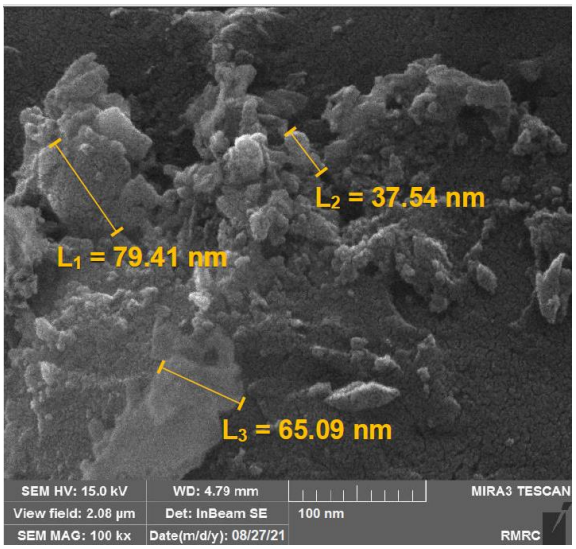

Fig. 3. The SEM images of TiO_2/Ag catalysts.

chloridazon as an active compound. The physical and chemical characteristics of chloridazon are shown in Table 1(Bike Ulu et al., 2020).

Synthesis of nanosized TiO_2/Ag

Methodology and synthesizing conditions are two main parameters that substantially determine the photocatalytic efficiencies of Ag/TiO_2 nanoparticles. Following are the major stages in the sol-gel method: (a) converting the alkoxides to metal hydroxides through using hydrolysis, (b) formation of gels by condensation process, and (c) drying to achieve Ag/TiO_2 photocatalyst. Typically, titanium tetrachloride ($TiCl_4$), tetrabutyl orthotitanate (TBOT), or titanium tetraisopropoxide (TIP) are titanium precursors, which combined with silver precursor (generally silver nitrate), accompanied by low temperature (less than 100 °C) hydrolysis. To provide homogeneous properties, the pH value should be monitored and regulated continuously during the synthesis process. Usually, for additional crystallization, some calcination process at high temperature is required because the sol-gel method commonly generates low crystalline or amorphous Ag/TiO_2 nanoparticles [19]. Ag/TiO_2 photocatalysts can be produced by the following equations (ethanol was utilized as solvent):

$$Ti(OH)_4 + C_2H_5O - Ag \rightarrow Ti(OH)_3 - Ag + C_2H_5OH \quad (1)$$

$$4Ti(OH)_3 - Ag + O_2 \rightarrow 4TiO_2 - AgNP + 6H_2O \quad (2)$$

The TiO_2/Ag nanoparticles were synthesized by a sol-gel method including a reduction agent. Silver nitrate and Titanium tetraisopropoxide were used as precursors of silver and titanium, respectively.

Sodium citrate tribasic dihydrate was applied as a reduction agent, and distilled water was employed in the tests. In a sealed four-way flask, about 2.0 mmol of $AgNO_3$ was mixed with 500mL of sodium citrate solution (4.0 mmol/L), and with continuous stirring, the temperature of the reaction was increased to 80 ◦C. The color of the solution was detected to switch from colorless to violet-brown signifying the reduction of silver. Formerly, 0.15 mol HNO_3 and 1 mol titanium tetraisopropoxide were added to the solution, and for 24 h it was continued at 50 ◦C to acquire TiO_2/Ag sol. The obtained sol was dried at 105 ◦C for 24 h and then it was calcined in the air between 300 and 700 ◦C for 2 h.

Batch photoreactor

As described in the previous work [20], the batch glass reactor with 25 cm in wide, 50 cm in length and 7 cm in height was used. The air was bubbled from the bottom into the reactor through a sparger. In all tests, the aeration rate was constant and uniform, and the magnet was placed in the middle of the reactor to stir the solution. Around the reactor was completely covered with insulation to prevent penetrating UV lights to outside. In addition, due to the high surface of the reactor and its low height, it was possible to diffuse oxygen uniformly throughout the reactor.

The conditions for all sampling were the same,

Table 2. Independent variables according to the CCD.

Factor	Factor Level				
	-2	-1	0	+1	+2
Chloridazon(mg/l) (A)	20	40	60	80	100
Catalyst Concentration(g/l)(B)	0.25	0.5	0.75	1.0	1.25
pH(C)	3.0	4.5	6	7.5	9.0
Treatment time(min)(D)	30	60	90	120	150

and all the solutions were exposed to ultraviolet

light without having a dead zone. The catalyst particles were suspended and slightly settled by stirring and aerating. The ultraviolet light source is a UV lamp from Philips Company in Holland with a length of 43 cm, a diameter of 2 cm, and a power of 15 w. This lamp is of low mercury pressure type. The lamp was placed horizontally above the reactor for the uniform radiation of the solution. The distance from the lamp to the surface of the reactor solution was 20 cm. The pH was adjusted by NaOH or HNO_3 (0.1 M) solution by PT-10P Sartorius pH meter.

Characterization tests

The structure of TiO_2 and TiO_2/Ag nanoparticles were recorded using X-ray powder diffraction (XRD) on a Philips instrument (X'pert diffractometer using CuKα radiation) at 25°C with a scanning speed at 0.03° (2θ) s^{-1}.

The morphology of the nano photocatalyst was characterized by FE-SEM (MIRA3TESCAN-XMU, FE-SEM) after gold coating. The concentration of CLZ was tested by HPLC technique Shimadzu, LC-20A Prominence, Japan with C18 column (250 mm × 4.6 mm), LC-20A solvent delivery unit, CBM 20A system controller, SIL 225 nm UV-VIS detector and 20A auto-sampler. Acetonitrile and ultra-pure water mobile phases were applied at 35% and 65% rates, respectively, with a fixed flow rate at 1 mL/min.

RESULTS AND DISCUSSION

FT-IR Analysis of TiO_2 and TiO_2/Ag nano photocatalyst

The molecular structure of the synthesized catalyst was characterized by FTIR spectra. The infrared spectrum of Ag/TiO_2 is measured by Perkin-Elmer FT-IR spectrophotometer with KBr pellets and illustrated in Fig. 1. As illustrated, the spectrum demonstrates the TiO_2 sample. The peak of Ti-O vibration is shown in the range of 4000-500 cm^{-1}. The peaks at 3400 cm^{-1} and 1637 cm^{-1} are related to O-H tensile and bending vibrations, respectively [21].

XRD results

The XRD patterns of synthesized TiO_2 and TiO_2/Ag 0.8 wt. % catalysts are demonstrated in Fig. 2. The peaks at 2θ = 24.8°, 37.3°, 48.2°, 54.4°, 56.3°, 63.0°, 70.5°, and 75.6° correspond to the anatase phase of the TiO_2 nanoparticles [22].

The diffraction peaks at 2θ = 38.1°, 44.3°, 64.4°, and 77.4° planes with face-centered cubic (FCC) are attributed to the Ag (JCPDS no 04-0783) [23]. But, the Ag/TiO_2 containing 0.8 wt. % did not show any peak that recommended Ag, because of its lower concentration.

The XRD patterns imply that the increasing silver content not only changes the crystalline size of the ultimate product but also accelerates titanium dioxide phase transfer from anatase to rutile. Rising the dopant dosage results in increasing the crystallite sizes. In addition, based on the outcomes, because of the grain-boundary pinning produced by dopant ions, 0.8 % of doped silver content might be optimal, which can regulate the development of crystallite and accumulation.

Moreover, based on XRD patterns, in contrast to bare titanium dioxide, which demonstrated the existence of both rutile and anatase phases, silver doping improves the anatase stability which is observed only in the XRD results of Ag/TiO_2 nanoparticles.

The XRD patterns of silver-doped TiO_2 photocatalyst annealed at 500 °C and proved the presence of anatase phase with no impurity in Ag or $AgNO_3$ phases and validated the absolute doping of silver in titanium dioxide. Moreover, it was detected that the crystallinity of silver-doped

Table 3. Design of experiments for each condition with their response (CLZ removal).

Std	Run	A: Chloridazon (mg. L^{-1})	B: Catalyst Concentration	C: pH	D: Treatment time (min)	Chloridazon Removal (%)
1	25	40	0.5	4.5	60	42.7
2	10	80	0.5	4.5	60	21.3
3	27	40	1	4.5	60	56
4	9	80	1	4.5	60	28
5	17	40	0.5	7.5	60	40.5
6	30	80	0.5	7.5	60	18.2
7	7	40	1	7.5	60	53
8	11	80	1	7.5	60	23.8
9	18	40	0.5	4.5	120	78.8
10	2	80	0.5	4.5	120	44
11	26	40	1	4.5	120	92
12	21	80	1	4.5	120	52.5
13	14	40	0.5	7.5	120	77.5
14	29	80	0.5	7.5	120	42.5
15	13	40	1	7.5	120	90.7
16	15	80	1	7.5	120	50
17	12	20	0.75	6	90	78.3
18	1	100	0.75	6	90	15.2
19	8	60	0.25	6	90	48.2
20	6	60	1.25	6	90	68.2
21	20	60	0.75	3	90	67.3
22	23	60	0.75	9	90	63.3
23	4	60	0.75	6	30	4.4
24	3	60	0.75	6	150	65.2
25	19	60	0.75	6	90	78.5
26	24	60	0.75	6	90	78
27	22	60	0.75	6	90	77.4
28	16	60	0.75	6	90	76.5
29	28	60	0.75	6	90	77.4
30	5	60	0.75	6	90	77.3

TiO_2 nanoparticles advanced with annealing temperature.

The crystal phase of the sample was recognized using XRD as shown in Fig. 2. The major phase of the synthesized nano photocatalyst is anatase.

The Crystallite size of pure TiO_2 was 20 nm, while the dimensions of Ag/TiO_2 nanoparticles were reported at about 60 nm.

The average crystalline size was achieved from the expansion of the main intense peak of anatase, by the Scherrer equation (Eq.3). The crystallite sizes (d) of synthesized nanoparticles were considered using the Scherrer formula, where λ is the wavelength of CuKα, θ is the Bragg's angle, and

Table 4. ANOVA tests in the removal of CLZ by TiO_2/Ag photo catalysts.

Source	S.S	DF	M. S.	F-value	p-value	
Model	16810.00	14	1200.71	3608.76	< 0.0001	significant
A-Chloridazon	5925.18	1	5925.18	17808.20	< 0.0001	
B-Catalyst Concentration	605.01	1	605.01	1818.36	< 0.0001	
C-pH	30.60	1	30.60	91.97	< 0.0001	
D-Treatment time	5584.55	1	5584.55	16784.42	< 0.0001	
AB	35.70	1	35.70	107.30	< 0.0001	
AC	0.7656	1	0.7656	2.30	0.1501	
AD	150.68	1	150.68	452.86	< 0.0001	
BC	0.5256	1	0.5256	1.58	0.2280	
BD	1.16	1	1.16	3.47	0.0821	
CD	2.18	1	2.18	6.54	0.0219	
A^2	1661.19	1	1661.19	4992.71	< 0.0001	
B^2	663.89	1	663.89	1995.33	< 0.0001	
C^2	271.26	1	271.26	815.28	< 0.0001	
D^2	3181.40	1	3181.40	9561.72	< 0.0001	
Residual	4.99	15	0.3327			
Lack of Fit	2.68	10	0.2682	0.5810	0.7827	not significant
Pure Error	2.31	5	0.4617			
Cor Total	16814.99	29				

β is the full width at half maxima of the diffraction peaks.

$$d = \frac{0.9\lambda}{\beta \cos\theta} \quad (3)$$

SEM results

The SEM image was employed to characterize the shape, size, and morphologies of the formed nanoparticle clusters. It displays the non-uniform aggregation of the Ag/TiO_2 nano photocatalyst, which results in a high surface area. The SEM images of the prepared Ag/TiO_2 nano photocatalyst are presented in Fig. 3. The SEM images of synthesized nanoparticles confirmed the homogenous spherical structure of TiO_2/Ag nanoparticles with a slightly aggregation of nanoparticles.

Experimental design

Typically, for the interpretation of complicated experimental designs, polynomial regression models are used. Since these models can appropriately extrapolate data besides offering simple functions for the prediction of variables. In the conditions where correlations between the variables and response values are obvious, through the application of regression models, the results must be statistically analyzed.

The CCD was employed to study the effect of initial concentration of CLZ (A), catalyst concentration (B), pH(C), and the treatment time on the removal of CLZ. The range of input parameters is shown in Table 2.

The CCD comprised axial points ($n_A = 8\,runs$) at distance α from the central point, a replicated central point ($n_C = 7\,runs$), and factorial points ($n_F = 16\,runs$) from a full 2^4 factorial design. A value of $\alpha = (n_F)^{\frac{1}{4}} = 2$, was taken to make the design rotatable [24].

To study the appropriateness of the model and evaluate the experimental error, replicates were used. Normally, the experimental design comprises 30 runs (Table 3) in random order to minimize the effects of inessential variables on the response.

In this study, the Design-Expert software version 10, (Stat-Ease Incorporation, USA, MN) was utilized for analyzing the experimental

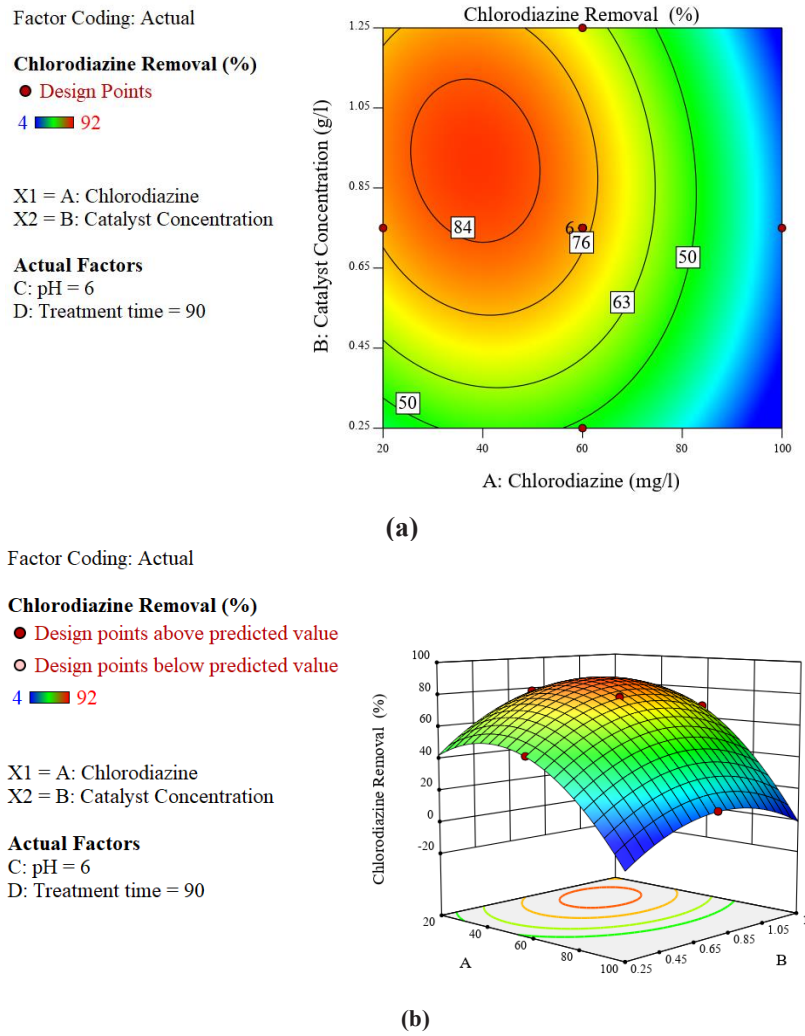

Fig. 4. (a) Contour plot, and (b) 3-D plots, for the influence of catalyst and CLZ concentration on CLZ degradation through TiO_2/Ag catalyst.

outcomes. For the prediction of response (Y) the polynomial equation (Eq.4) was recommended by the software as a function of independent variables.

$$Y = \beta_0 + \sum_{i=1}^{4} \beta_i x_i + \sum_{i=1}^{4} \beta_{ii} x_i^2 + \sum_{i=1}^{4} \sum_{j=1,i<j}^{4} \beta_{ij} x_i x_j \quad (4)$$

Table 3 demonstrated the experimental outcomes for independent variables and the response values. Where, β_0 is a constant coefficient, β_i coefficient of linear effect, β_{ii} is the coefficient of quadratic or squared effect, β_{ij} is representing the coefficient of interactions effect, x_i is the coded independent parameters and Y is the response value.

If there is a relation between the factors and response, the achieved data should be analyzed statistically by regression.

Analysis of variance (ANOVA)

For investigation and optimization of influential major parameters on the CLZ removal effectiveness, the response surface methodology (RSM) was used. As was shown in Table 4, the ANOVA results were used to explore the interaction between each independent variable and response. As it was depicted in the ANOVA Table, the model p-value was determined at 0.05. The F-value is an indication of model significance. In the conditions where the calculated F-value is higher than F-value, the p-value will be remarkably decreased which implies the model significance. According to the ANOVA results, the F-value of 167.06 confirmed that the model is highly robust towards the effect of noise. In other words, the feasibility of happening such a large F-value due to noise is only 0.01% [25].

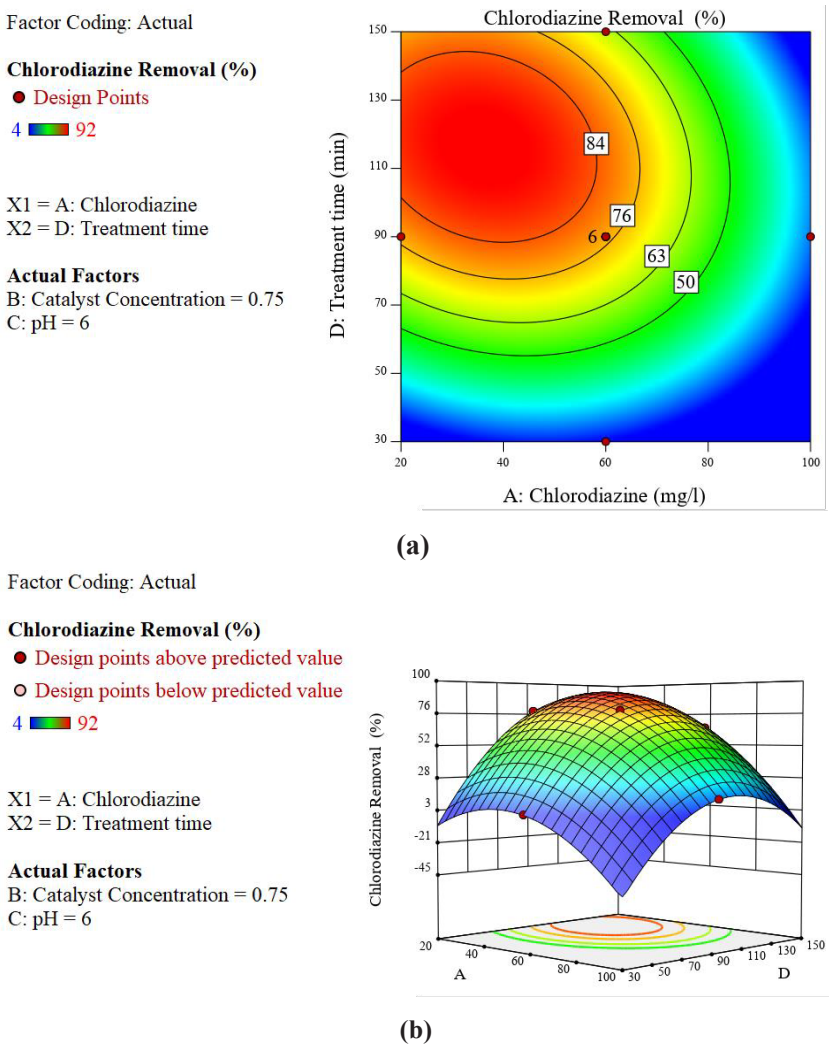

Fig. 5. (a) Contour plot, and (b) 3-D plots, for the influence of treatment time and CLZ concentration on CLZ degradation through TiO_2/Ag catalyst.

As a widely accepted criterion, the p-values lower than 0.05 are an indication of the significance of that term. In the current work, A, B, C, D, AB, CD, AC, BD, A^2, B^2, and C^2 are significant model terms and in contrast AD, CD, and BD are considered as insignificant model terms because their p-values go beyond mentioned criterion. When there is a lot of insignificant model terms (except those required to maintain the hierarchy of the model), the reduction can improve the efficiency of the model.

The Model F-value of 3608.76 indicates the model is highly significant and the possibility of occurring such a large F-value because of noise is only 0.01%. In the current study, A, B, C, D, AB, AD, CD, A^2, B^2, C^2, D^2 are significant model terms because they have p-values less than 0.05. Also, p-values higher than 0.1 imply that model terms are insignificant. In the case of many insignificant model terms (without considering those terms which must be present for maintaining model hierarchy), for enhancing statistical parameters of the model, the model reduction would be a suitable approach. The "Lack of Fit" is the quantity that the model predictions miss the observations. It is measured by comparing residual error with pure error from the replicated design points, which usually are the central points in the experiment. If the lack of fit value goes beyond F-value, it is implied that there is a fault in the lack of fit, and as a result the regression model needs improvement. In this vein, the F-value of lack of fit at 0.58 indicates that the lack of fit is significant and the possibility of occurring such a large F-value for lack of fit is 78.27% because of noise. Always, insignificant lack

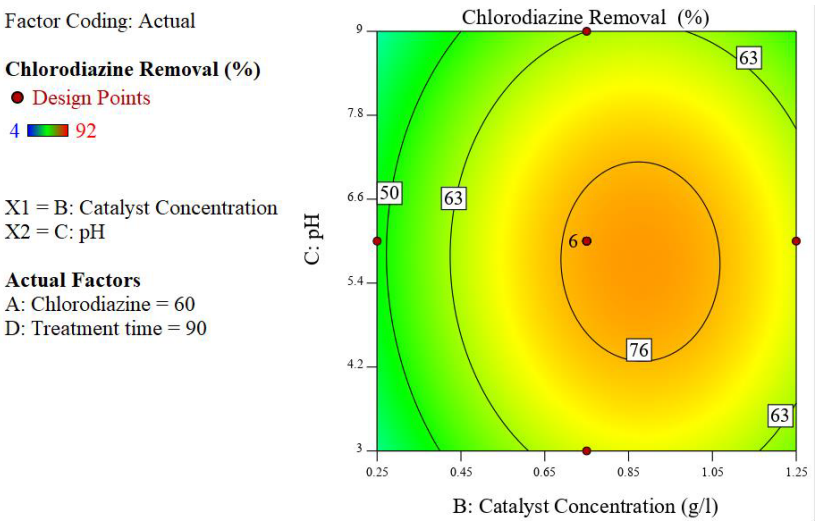

(a)

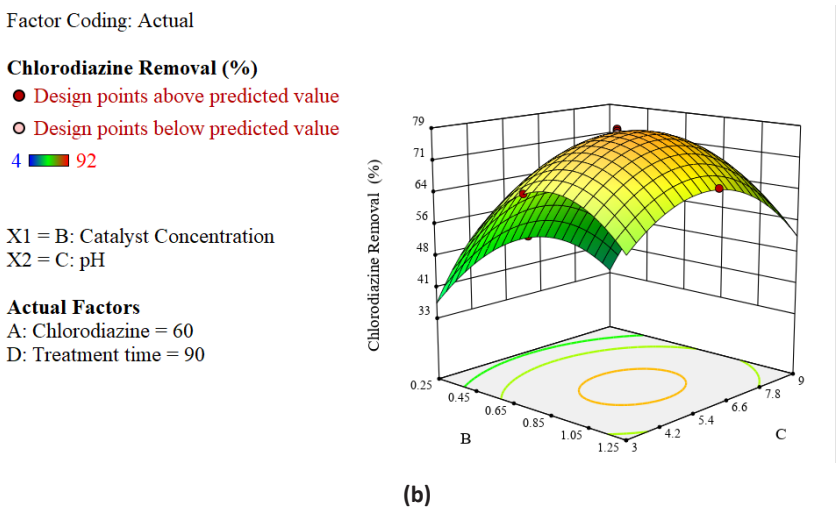

(b)

Fig. 6. a) Contour plot, and b) 3-D plots, for the influence of pH and catalyst concentration on CLZ degradation by TiO_2/Ag photocatalyst.

of fit values is desirable.

The Adj.R^2 of 0.9994 and the Pred.R^2 of 0.9989 are in good harmony with each other because their difference is less than 0.2. The signal-to-noise ratio was calculated by adequate precision and a ratio higher than 4 is favorable. The adequate precision of 217.009 demonstrates a proper quantity of signal. As a result, this model can be utilized for the navigation of experimental design space. To anticipate response values for particular levels of each parameter, the coded equation can be utilized. The high and low levels of each variable are coded by +1 and -1, respectively. Through a comparison of coefficients of each variable, their relevant effect on the response can be recognized.

Moreover, because increasing the values of the sum of squares results in an increase in the significance of parameters as a result, for determining the significance of a given variable, the sum of squares must be explored [26]. Based on the outcomes, Eq.5 was presented the anticipated response equation (second-order polynomial).

$$\text{removal of clz(\%)} = +77.52 - 15.71A + 5.02B - 1.13C + 15.25D - 1.49AB - 0.2187AC - 3.07AD - 0.1812BC + 0.2688BD + 0.3688CD - 7.78A^2 - 4.92B^2 - 3.14C^2 - 10.77D^2 \quad (5)$$

Moreover, through using the original units of each parameter for their given level in the actual equation, the anticipation of response values can be performed. Since coefficients are scaled to adapt

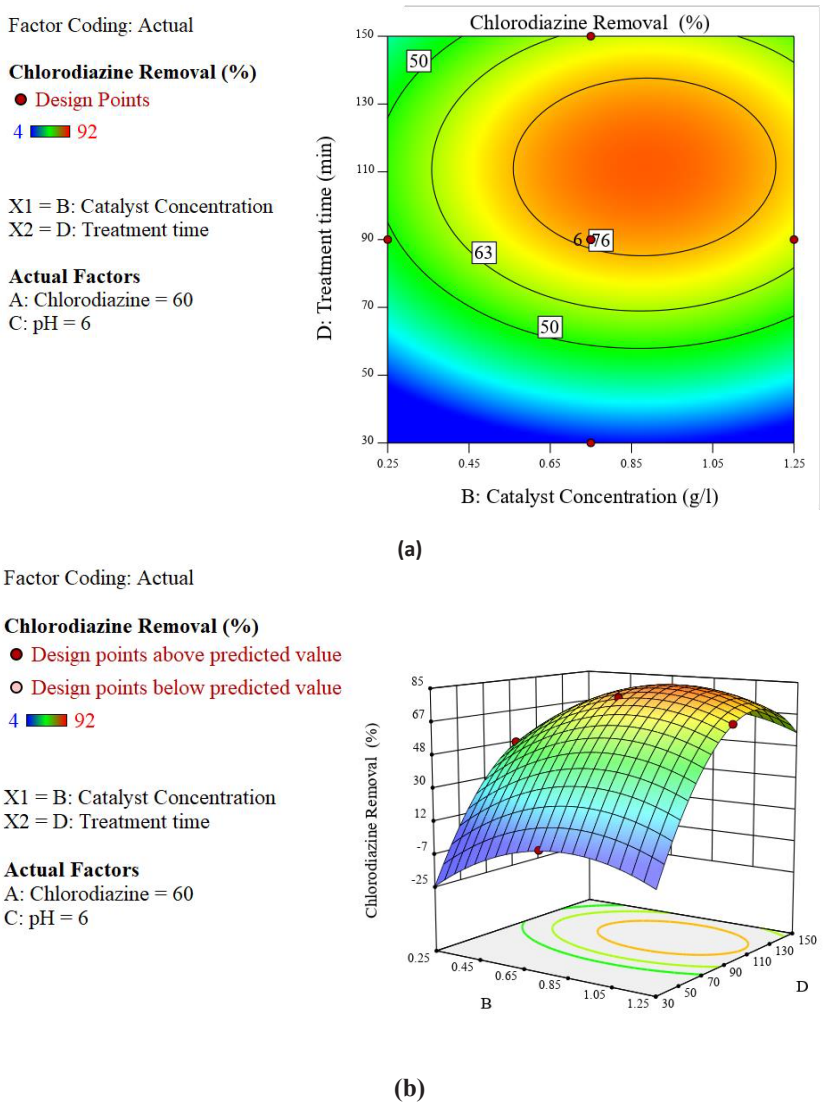

Fig. 7. a) Contour plot, and b) 3-D plots, for the influence of treatment time and catalyst concentration on CLZ degradation through TiO_2/Ag catalyst.

the units of each variable, the actual equation cannot be utilized to ascertain their effect on the response [27].

Effect of initial concentration of TiO_2/Ag

The influence of TiO_2/Ag dosage on CLZ degradation is shown in Fig. 4. As shown, the CLZ degradation percentage was improved to some extent and after that, an increase in catalyst dosage did not change the degradation efficacy notably. Enhance in catalyst dosage increased the interaction between catalyst and chloridazon herbicide which increased the degradation efficiency of CLZ.

Therefore, the catalyst dosage at 0.83gr/l was selected as optimum catalyst dosage to remove CLZ in synthetic wastewater.

The influence of silver dosage on the ultimate characteristics of the Ag/TiO_2 nanocatalyst was explored by Mogal et al. [28]. Using a single-step sol-gel route through dissolving Ag and Ti precursors with ammonia and methanol, the silver-doped TiO_2 nanoparticles with 0.8 wt % of silver were synthesized.

Influence of initial CLZ concentration

The influence of CLZ initial concentration on the degradation of CLZ using TiO_2/Ag catalyst is illustrated in Fig. 5. As shown, the time needed for complete degradation of CLZ using TiO_2/Ag catalyst was increased with increase in initial

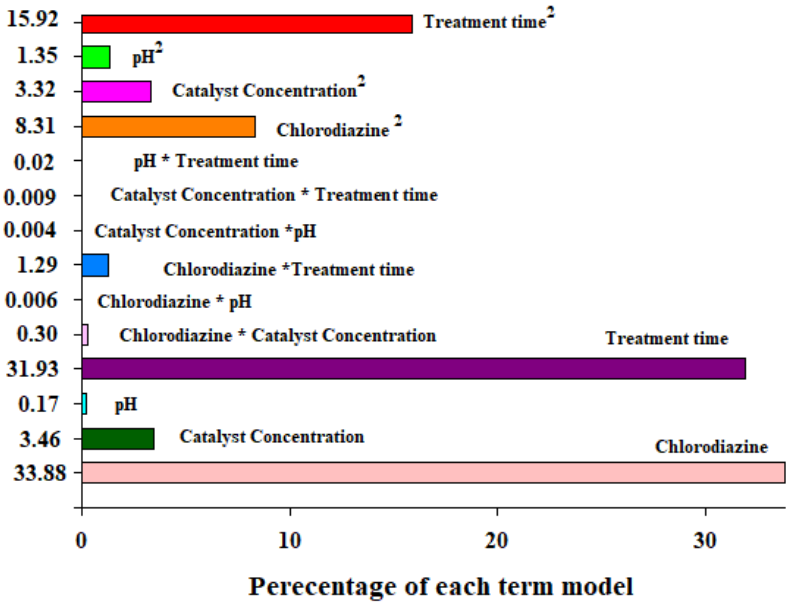

Fig. 8. Pareto chart for operational variables in CLZ removal.

CLZ concentration. Furthermore, enhancement in CLZ concentration results in a decrease in the degradation rate of the CLZ. In higher concentrations of CLZ, due to the limited number of requirements of reactive species for reaction with CLZ, more time was needed for complete degradation of CLZ. Further increase in pollutant concentration led to a decrease in degradation efficiency.

As the concentration of CLZ increased, more pesticide molecules reacted with available active sites consequently, the degradation rate increased. But the high concentration of CLZ, acts as a filter for the incident light, which decreases the formation of hydroxyl radicals, and subsequently degradation efficiency [29].

Effect of initial pH on degradation of CLZ

In an aqueous medium, the adsorbent capacity is influenced by pH via changing the surface properties of the adsorbent. The rate of photocatalytic degradation of CLZ was slightly higher in the neutral and slightly acidic pH range as shown in Fig. 6. This behavior is due to the increase in the photocatalytic degradation rate due to the improved availability of hydroxyl radicals. The adsorption on Ag-TiO_2 is due to surface features and reactivity mainly originating from the surface hydroxyl groups.

The effect of pH on CLZ degradation using TiO_2/Ag photocatalysts in the range of 3 to 9 is shown in Fig. 6. As shown, the maximum degradation of CLZ occurred at pH of 6.8 using TiO_2/Ag catalysts. Chloridazon has a pK_a= 1. At pH above 1, the chloridazon herbicide has a negative charge. On the other hand, the point of zero charges (PZC) of TiO_2/Ag catalyst is about 6 [30]. Therefore, the positive holes are considered as the main oxidation stage at pH lower than 6, while hydroxyl radicals are considered as the principal species at pH upper than 6 [31]. The pH of 6.8 is considered as an optimal pH value in CLZ degradation.

Influence of treatment time on degradation of chloridazon

The degradation time is a very important variable in designing the photocatalytic process. The influence of reaction time on degradation of CLZ using TiO_2/Ag catalysts for 60 mg L^{-1} of initial CLZ concentration at 25°C is shown in Fig. 7. It was clear that after 115 min, the active sites of catalyst were saturated, and then the degradation rate was reduced due to the adsorption of CLZ by intra-particular sites of TiO_2/Ag catalysts. Almost the internal and external active sites of TiO_2/Ag catalysts were saturated at the end of reaction.

The synthesized TiO_2/Ag particles were washed with distilled water and ethanol and reused three times for degradation of CLZ from an aqueous environment. The chloridazon removing

percentage did not significantly change after three times. The gained results showed the high capacity of TiO_2/Ag catalyst in practical processes [32].

The Pareto charts

An operative statistical-based technique to investigate the synchronized influence of parameters is RSM. The Pareto chart was analyzed to identify the significant variables that affect the response. The influences of experimental variables on the response at optimum conditions in contour plots and three-dimensional response surfaces (Figs.4-7) were envisioned thru Pareto charts (Fig. 8).

The graphical Pareto chart is performed to show the effect of each operative variable on the response and evaluated by the resulting equation (Eq.6).

$$P_i = (\frac{b_i^2}{\sum b_i^2}) \times 100 \qquad (6)$$

The term b_i signifies the effect of the numerical coefficient for each variable. The concentration of CLZ and pH were the significant parameters that impact the removal of CLZ. Other researchers attained parallel results via a Pareto chart [33].

CONCLUSION

This study describes the synthesis of TiO_2 and TiO_2/Ag catalysts via the sol-gel method. The prepared catalysts were used for the removal of chloridazon along with UV irradiation. FE-SEM analysis showed the synthesis of uniform TiO_2 and TiO_2/Ag composite. The Crystallite size of pure TiO_2 and Ag/TiO_2 nanoparticles was 20 and 60 nm, respectively. The obtained results showed that the Ag/TiO_2 nano photocatalyst had a higher efficiency in degradation of CLZ compared to TiO_2.

The CCD was employed to study the removal of CLZ in an aqueous environment. The effect of four critical, independent parameters, including the initial concentration of CLZ, treatment time, pH, and catalyst dosage on the response has been explored. The optimal conditions for each critical variable were as the following: time at 113 min, pH at 6.8, initial concentration of CLZ at 40 mg/l, and 0.83gr/l of catalyst. The maximum effectiveness in the experimental and predicted CLZ removal was 94.2 and 93.5%, respectively. The outcomes of ANOVA demonstrated high determination coefficient quantities (R^2 = 0.9997, Predicted R^2=0.9989, and Adjusted R^2=0.9994) which validated the reliability of the second-order regression model. In order to interpret the influence of each parameter besides their interactions on each other, the contour and 3-D plots were utilized.

CONFLICT OF INTEREST

The authors declare no conflict of interest.

REFERENCES

1 M. Hadei, A. Mesdaghinia, R. Nabizadeh, A.H. Mahvi, S. Rabbani, K. Naddafi, Environ. Sci. Pollut. Res. 28: 13055 (2021). https://doi.org/10.1007/S11356-021-12576-8. https://doi.org/10.1007/s11356-021-12576-8

2 F. Yan, S. Kumar, K. Spyrou, A. Syari'ati, O. De Luca, E. Thomou, E.M. Alfonsín, D. Gournis, P. Rudolf, ACS Environ. Sci. Technol. Water. 1: 157 (2021). https://doi.org/10.1021/ACSESTWATER.0C00037/SUPPL_FILE/EW0C00037_SI_001.PDF https://doi.org/10.1021/acsestwater.0c00037

3 A. Mbiri, G. Wittstock, D.H. Taffa, E. Gatebe, J. Baya, M. Wark, Environ. Sci. Pollut. Res. 25: 34873 (2017). https://doi.org/10.1007/S11356-017-1023-X. https://doi.org/10.1007/s11356-017-1023-x

4 F. Yan, K. Spyrou, E. Thomou, S. Kumar, H. Cao, M.C.A. Stuart, Y. Pei, D. Gournis, P. Rudolf, Environ. Sci. Nano. 7: 424 (2020). https://doi.org/10.1039/C9EN00974D. https://doi.org/10.1039/C9EN00974D

5 J. Zhao, Z. Chi, H. Dong, C. Sun, H. Yu, H. Yu, -J. Clean. Prod., 300, 2021, 126961, https://doi.org/10.1016/j.jclepro.2021.126961. https://doi.org/10.1016/j.jclepro.2021.126961

6 H. Azaari, R. Chahboune, M. El Azzouzi, M. Sarakha, Rapid Commun. Mass Spectrom. 30: 1145 (2016). https://doi.org/10.1002/RCM.7541. https://doi.org/10.1002/rcm.7541

7 A. Shokri, M. Salimi, T. Abmatin, Fresenius Environ. Bull. 26: 1560 (2017).

8 M. Rostami, H. Mazaheri, A. Hassani Joshaghani, A. Shokri, Int. J. Eng. Trans. B Appl. 32: 1074 (2019). https://doi.org/10.5829/ije.2019.32.08b.03. https://doi.org/10.5829/ije.2019.32.08b.03

9 S. Abbad, K. Guergouri, S. Gazaout, S. Djebabra, A. Zertal, R. Barille, M. Zaabat, J. Environ. Chem. Eng. 8: 103718 (2020). https://doi.org/10.1016/J.JECE.2020.103718. https://doi.org/10.1016/j.jece.2020.103718

10 Z. Sarteep, A. Ebrahimian Pirbazari, M.A. Aroon, J. Water Environ. Nanotechnol. 1: 135 (2016). https://doi.org/10.7508/JWENT.2016.02.007.

11 X. Zheng, D. Zhang, Y. Gao, Y. Wu, Q. Liu, X. Zhu, Inorg. Chem. Commun. 110: 107589 (2019). https://doi.org/10.1016/J.INOCHE.2019.107589. https://doi.org/10.1016/j.inoche.2019.107589

12 D. Chen, Q. Chen, L. Ge, L. Yin, B. Fan, H. Wang, H. Lu, H. Xu, R. Zhang, G. Shao, Appl. Surf. Sci. 284: 921 (2013). https://doi.org/10.1016/J.APSUSC.2013.08.051. https://doi.org/10.1016/j.apsusc.2013.08.051

13 S.Y. Ryu, J.W. Chung, S.Y. Kwak, Compos. Sci. Technol. 117: 9 (2015). https://doi.org/10.1016/J.COMPSCITECH.2015.05.014. https://doi.org/10.1016/j.compscitech.2015.05.014

14 M. Bingham, A. Mills, J. Photochem. Photobiol. A: Chem. 389, 2020, 112257, https://doi.org/10.1016/j.jphotochem.2019.112257.

https://doi.org/10.1016/j.jphotochem.2019.112257
15 A. Shokri, S. Karimi, J. Water Environ. Nanotechnol. 6: 326 (2021). https://doi.org/10.22090/jwent.2021.04.004.
16 A. Khanna, V. Shetty K, New Pub Balaban. 54: 744 (2014). https://doi.org/10.1080/19443994.2014.888681. https://doi.org/10.1080/19443994.2014.888681
17 K. Tahir, A. Ahmad, B. Li, S. Nazir, A.U. Khan, T. Nasir, Z.U.H. Khan, R. Naz, M. Raza, J. Photochem. Photobiol. B Biol. 162: 189 (2016). https://doi.org/10.1016/J.JPHOTOBIOL.2016.06.039. https://doi.org/10.1016/j.jphotobiol.2016.06.039
18 K.H. Leong, B.L. Gan, S. Ibrahim, P. Saravanan, Appl. Surf. Sci. 319: 128 (2014). https://doi.org/10.1016/J.APSUSC.2014.06.153. https://doi.org/10.1016/j.apsusc.2014.06.153
19 M. Sharma, M. Pathak, P.K., A.J. Chem. 30: 1405 (2018). https://doi.org/10.14233/ajchem.2018.20845 https://doi.org/10.14233/ajchem.2018.20845
20 R. Hekmatshoar, A.R. Yari, A. Shokri, J. Nanoanalysis. 7:10 (2020). https://doi.org/10.22034/jna.
21 M. Rostami, A. Hassani Joshaghani, H. Mazaheri, A. Shokri, Int. J. Eng. Trans. A Basics. 34: 756 (2021). https://doi.org/10.5829/ije.2021.34.04a.01. https://doi.org/10.5829/ije.2021.34.04a.01
22 K.H. Leong, P. Monash, S. Ibrahim, P. Saravanan, Sol. Energy. 101: 321 (2014). https://doi.org/10.1016/J.SOLENER.2014.01.006. https://doi.org/10.1016/j.solener.2014.01.006
23 Y. Liu, Q. Zhang, M. Xu, H. Yuan, Y. Chen, J. Zhang, K. Luo, J. Zhang, B. You, Appl. Surf. Sci. 476: 632 (2019). https://doi.org/10.1016/J.APSUSC.2019.01.137. https://doi.org/10.1016/j.apsusc.2019.01.137
24 A. Shokri, Desalin. Water Treat. 247: 92 (2022). https://doi.org/10.5004/dwt.2022.28037. https://doi.org/10.5004/dwt.2022.28037
25 A.Shokri, Surf. Interfaces, 21:100705(2020). https://doi.org/10.1016/j.surfin.2020.100705
26 A. Shokri, H. Moradi, M. Abdouss, B. Nasernejad, Desalin.Water Treat, 205:264 (2020). https://doi.org/10.5004/dwt.2020.26384
27 A. Shokri, A. Bayat, K. Mahanpoor, Desalin. Water Treat. 166: 135 (2019). https://doi.org/10.5004/dwt.2019.24634. https://doi.org/10.5004/dwt.2019.24634
28 S.I. Mogal, V.G. Gandhi, M. Mishra, S. Tripathi, T. Shripathi, P.A. Joshi, D.O. Shah, Ind. Eng. Chem. Res. 53: 5749 (2014). https://doi.org/10.1021/IE404230Q/SUPPL_FILE/IE404230Q_SI_001.PDF. https://doi.org/10.1021/ie404230q
29 M. Saghi, A. Shokri, A. Arastehnodeh, M. Khazaeinejad, A. Nozari, J. Nanoanalysis. 5: 163 (2018). https://doi.org/10.22034/JNA.2018.543608.
30 H. Bike Ulu, N. Değermenci, F.B. Dilek, 194:429 (2020). https://doi.org/10.5004/dwt.2020.25905. https://doi.org/10.5004/dwt.2020.25905
31 K.A. Razak, D. Suriyani, C. Halin, M.M. Al, B. Abdullah, M. Arif, A.M. Salleh, Trans Tech Publ. 280:26 (2018). https://doi.org/10.4028/www.scientific.net/SSP.280.26. https://doi.org/10.4028/www.scientific.net/SSP.280.26
32 A. Shokri, Environ. Challenges. 5: 100332 (2021). https://doi.org/10.1016/j.envc.2021.100332. https://doi.org/10.1016/j.envc.2021.100332
33 A. Shokri, Chemosphere. 296: 133817 (2022). https://doi.org/10.1016/J.CHEMOSPHERE.2022.133817. https://doi.org/10.1016/j.chemosphere.2022.133817